J|A|C|S ARTICLES

Published on Web 02/12/2010

Phenylacetylene One-Dimensional Nanostructures on the Si(100)-2 × 1:H Surface

Michael A. Walsh,[†] Stephanie R. Walter,[‡] Kirk H. Bevan,[§,||] Franz M. Geiger,[‡] and Mark C. Hersam*[,†,‡]

Department of Materials Science and Engineering, Northwestern University, Evanston, Illinois 60208, Department of Chemistry, Northwestern University, Evanston, Illinois 60208, Materials Science and Technology Division, Oak Ridge National Laboratory, Oak Ridge, Tennessee 37831, and Centre for the Physics of Materials and Department of Physics, McGill University, Montreal, PQ, H3A 2T8, Canada

Received October 27, 2009; E-mail: m-hersam@northwestern.edu

Abstract: Using ultrahigh vacuum (UHV) scanning tunneling microscopy (STM), many olefins have been shown to self-assemble on the hydrogen-passivated Si(100)-2 × 1 surface into one-dimensional nanostructures. This paper demonstrates that similar one-dimensional nanostructures can also be realized using alkynes. In particular, UHV STM, sum frequency generation (SFG), and density functional theory (DFT) are employed to study the growth mechanism and binding configuration of phenylacetylene (PA) one-dimensional nanostructures on the Si(100)-2 × 1:H surface. Molecular-resolution UHV STM images reveal the binding position and spacing of PA with respect to the underlying silicon dimer rows. Furthermore, UHV STM characterization of heteromolecular one-dimensional nanostructures of styrene and PA shows distinct electronic contrast between the two molecules, which is confirmed using simulated STM images derived from DFT and provides insight into the nature of PA binding to silicon. Additional evidence from SFG measurements corroborates the conclusion that the terminal carbon atoms of PA retain π-conjugation following reaction to the Si(100)-2 × 1:H surface.

Introduction

Ultrahigh vacuum (UHV) scanning tunneling microscopy (STM) studies of silicon functionalized with organic molecules have received great attention in the fields of molecular electronics and biological and chemical sensing.[1−4] Hydrogen-passivated silicon is a particularly interesting substrate since UHV STM allows nanopatterning of organic molecules down to the single-molecule level on this surface.[5−9] Some molecules, typically olefins, have been shown to self-assemble via a radical-mediated growth mechanism into one-dimensional molecular nanostructures aligning parallel[10] or perpendicular[11] to the silicon dimer row on the hydrogen-passivated surface. Chain-growing molecules with different functionalities[10−20] and binding configurations[21] and their interactions with organic[9,22,23] and inorganic[24] nanostructures have been thoroughly investigated. The molecules studied thus far all share a similar self-assembly reaction mechanism in which the molecule is covalently bound to the silicon surface with sp^3 hybridization. On the other hand, molecules with a terminal acetylene group have the potential

[†] Department of Materials Science and Engineering, Northwestern University.
[‡] Department of Chemistry, Northwestern University.
[§] Oak Ridge National Laboratory.
[||] McGill University.

(1) Wolkow, R. A. *Annu. Rev. Phys. Chem.* **1999**, *50*, 413–441.
(2) Hersam, M. C.; Guisinger, N. P.; Lyding, J. W. *Nanotechnology* **2000**, *11*, 70–76.
(3) Buriak, J. M. *Chem. Rev.* **2002**, *102*, 1271–1308.
(4) Hersam, M. C.; Reifenberger, R. G. *MRS Bull.* **2004**, *29*, 385–390.
(5) Walsh, M. A.; Hersam, M. C. *Annu. Rev. Phys. Chem.* **2009**, *60*, 193–216.
(6) Abeln, G. C.; Lee, S. Y.; Lyding, J. W.; Thompson, D. S.; Moore, J. S. *Appl. Phys. Lett.* **1997**, *70*, 2747–2749.
(7) Abeln, G. C.; Hersam, M. C.; Thompson, D. S.; Hwang, S. T.; Choi, T.; Moore, J. S.; Lyding, J. W. *J. Vac. Sci. Technol. B* **1998**, *16*, 3874–3878.
(8) Hersam, M. C.; Guisinger, N. P.; Lyding, J. W. *J. Vac. Sci. Technol. A* **2000**, *18*, 1349–1353.
(9) Basu, R.; Guisinger, N. P.; Greene, M. E.; Hersam, M. C. *Appl. Phys. Lett.* **2004**, *85*, 2619–2621.
(10) Lopinski, G. P.; Wayner, D. D. M.; Wolkow, R. A. *Nature* **2000**, *406*, 48–51.
(11) Hossain, Z.; Kato, H. S.; Kawai, M. *J. Am. Chem. Soc.* **2005**, *127*, 15030–15031.
(12) Kruse, P.; Johnson, E. R.; DiLabio, G. A.; Wolkow, R. A. *Nano Lett.* **2002**, *2*, 807–810.
(13) DiLabio, G. A.; Piva, P. G.; Kruse, P.; Wolkow, R. A. *J. Am. Chem. Soc.* **2004**, *126*, 16048–16050.
(14) Kirczenow, G.; Piva, P. G.; Wolkow, R. A. *Phys. Rev. B* **2005**, *72*, 245306.
(15) Pitters, J. L.; Dogel, I.; DiLabio, G. A.; Wolkow, R. A. *J. Phys. Chem. B* **2006**, *110*, 2159–2163.
(16) Basu, R.; Kinser, C. R.; Tovar, J. D.; Hersam, M. C. *Chem. Phys.* **2006**, *326*, 144–150.
(17) Hossain, M. Z.; Kato, H. S.; Kawai, M. *J. Am. Chem. Soc.* **2007**, *129*, 3328–3332.
(18) Hossain, M. Z.; Kato, H. S.; Kawai, M. *J. Am. Chem. Soc.* **2007**, *129*, 12304–12309.
(19) Hossain, M. Z.; Kato, H. S.; Kawai, M. *J. Am. Chem. Soc.* **2008**, *130*, 11518–11523.
(20) Hossain, M. Z.; Kato, H. S.; Kawai, M. *J. Phys. Chem. C* **2009**, *113*, 10751–10754.
(21) Walsh, M. A.; Hersam, M. C. *Chem. Commun.* **2010**, *46*, 1153–1155.
(22) Pitters, J. L.; Wolkow, R. A. *J. Am. Chem. Soc.* **2005**, *127*, 48–49.
(23) Hossain, M. Z.; Kato, H. S.; Kawai, M. *J. Phys. Chem. B* **2005**, *109*, 23129–23133.
(24) Wang, Q. H.; Hersam, M. C. *J. Am. Chem. Soc.* **2008**, *130*, 12896–12897.

for undergoing one-dimensional chain reactions such that the resulting nanostructures possess conjugated sp^2 hybridization at the surface. A structure of this type is likely to be of interest for molecular electronics and sensing applications since extended π-conjugation is known to enhance electronic coupling and facilitate charge transport.[25−28]

Self-assembled monolayers of alkynes, such as phenylacetylene (PA), have previously been investigated on wet chemically passivated Si(111):H and Si(100):H. Studies of the monohydride Si(111) case reveal that the sp^2 hybridization of the terminal carbon atoms is retained,[29−31] while studies of the mixed-hydride Si(100) case present evidence of a secondary surface reaction occurring in which the sp^2 hybridization is lost and the molecule is bound at multiple sites with sp^3 hybridization.[32] The UHV-prepared monohydride Si(100)-2 × 1:H surface shares characteristics with both surfaces, and thus, the binding configuration for PA is not self-evident.

This manuscript reports UHV STM, sum frequency generation (SFG), and density functional theory (DFT) studies of PA molecules on the Si(100)-2 × 1:H surface. Constant current STM imaging reveals that PA forms one-dimensional nanostructures with molecular spacing and position that are consistent with previous observations for styrene. However, additional STM images of heteromolecular one-dimensional nanostructures of styrene and PA reveal apparent height contrast, which suggests differences in the electronic structure between the two molecules, which is confirmed through DFT calculations. Finally, SFG provides corroborating spectroscopic evidence that the terminal PA carbon atoms possess sp^2 hybridization following covalent reaction to the Si(100)-2 × 1:H surface. Overall, these studies demonstrate that PA molecules form highly conjugated one-dimensional nanostructures on the Si(100)-2 × 1:H surface.

Experimental Details

Materials. Phenylacetylene (98%, Sigma Aldrich), styrene (≥99%, Sigma Aldrich), phenyl-d_5-acetylene (99.2%, 99.6% D, CDN Isotope), and styrene-2,3,4,5,6-d_5 (98.3%, 99% D, CDN Isotopes) were used as received. All molecules were loaded into glass vials housed on a manifold that was connected to the UHV STM chamber through a controlled leak valve. Prior to loading, each vial was cleaned with acetone and isopropanol and baked in an oven at 400 K for several hours. The vials were then mounted to the manifold where they were heated with an acetylene torch while being evacuated by a turbomolecular pump. Following cleaning, the vials were loaded with the respective molecules in a controlled atmosphere nitrogen glovebox (<1 ppm H_2O and O_2) and mounted back on the manifold, where they underwent several freeze−pump−thaw cycles preceding introduction to UHV.

Hydrogen Passivation. The Si(100) sample preparation was performed in a home-built two-chamber UHV system with separate chambers for sample preparation and STM at an operating base pressure of 5.0×10^{-11} Torr.[33] The silicon used for the experiments was cut from an n-type Si(100) wafer (VA Semiconductor, As doped, <0.005 Ω-cm) and degreased by ultrasonication in acetone and isopropanol for 5 min each. The samples were then introduced into the UHV system via a load lock and degassed for several hours at 900 K. The samples were flashed several times at 1500 K to form the clean Si(100)-2 × 1 surface prior to passivation. For the UHV STM experiments, the samples were passivated by resistively heating the substrate to ∼650 K and backfilling the chamber with molecular hydrogen. The hydrogen gas was cracked on a hot tungsten filament (1600 K) located approximately 6 cm from the sample face. Overall, the silicon sample was exposed to 3000 Langmuirs (1 Langmuir = 1×10^{-6} Torr s) of hydrogen. The hydrogen passivation for the SFG experiments followed the same procedure except the sample was heated to ∼675 K in order to increase the coverage of silicon dangling bond (DB) sites on the surface. The surface quality was confirmed by UHV STM imaging using either electrochemically etched W or commercially available PtIr (Agilent Technologies) probes. Additionally, the DB coverage was determined using UHV STM by scanning over many different areas and counting the number of DBs on the surface.

Molecular Dosing. For UHV STM experiments of PA-functionalized Si(100)-2 × 1:H, the sample was subjected to a dose of PA between 5 and 30 Langmuirs via a controlled leak valve. In the case of UHV STM experiments with heteromolecular nanostructures of styrene and PA, the surface was initially dosed with 30 Langmuirs of styrene and imaged to ensure surface quality. The sample was then exposed to a 60 Langmuir dose of PA.

The SFG experiments required two alterations to the molecular dosing procedure. First, in order to avoid spectral interference in the SFG signal from the phenyl group of the PA and styrene molecules, phenyl-d_5-acetylene (PA-d) and styrene-2,3,4,5,6-d_5 (sty-d) molecules with deuterated phenyl groups were used. Second, in order to ensure a strong signal from the SFG measurement, a high coverage of sty-d and PA-d was needed. To accomplish the high coverage, the Si(100)-2 × 1:H samples were hydrogen passivated at 675 K as described above and then dosed with 180 Langmuirs of the sty-d molecule or 300 Langmuirs of the PA-d molecule, which achieved an approximate coverage of 0.1 monolayers. Following molecular dosing, the samples were stored in either UHV or a controlled atmosphere nitrogen glovebox (<1 ppm H_2O and O_2).

Scanning Tunneling Microscopy. UHV STM analysis was carried out using a home-built microscope with a dual concentric piezotube design.[33] All topographic imaging was performed in constant current mode. The bias voltage was applied to the sample with respect to the STM tip that was grounded through a current preamplifier.

Sum Frequency Generation. Complete descriptions of the theoretical and experimental aspects of sum frequency generation (SFG) are provided in the literature.[34−39] The laser system used for these SFG experiments has been detailed previously.[40−45] Briefly, an 800 nm, 120 fs regeneratively amplified Ti:Sapphire

(25) Mantooth, B. A.; Weiss, P. S. *Proc. IEEE* **2003**, *91*, 1785–1802.
(26) Hacker, C. A.; Hamers, R. J. *J. Phys. Chem. B* **2003**, *107*, 7689–7695.
(27) Pluchery, O.; Coustel, R.; Witkowski, N.; Borensztein, Y. *J. Phys. Chem. B* **2006**, *110*, 22635–22643.
(28) Saito, N.; Hayashi, K.; Sugimura, H.; Takai, O. *Langmuir* **2003**, *19*, 10632–10634.
(29) Linford, M. R.; Fenter, P.; Eisenberger, P. M.; Chidsey, C. E. D. *J. Am. Chem. Soc.* **1995**, *117*, 3145–3155.
(30) Cicero, R. L.; Linford, M. R.; Chidsey, C. E. D. *Langmuir* **2000**, *16*, 5688–5695.
(31) Kellar, J. A.; Lin, J. C.; Kim, J. H.; Yoder, N. L.; Bevan, K. H.; Stokes, G. Y.; Geiger, F. M.; Nguyen, S. T.; Bedzyk, M. J.; Hersam, M. C. *J. Phys. Chem. C* **2009**, *113*, 2919–2927.
(32) Sieval, A. B.; Opitz, R.; Maas, H. P. A.; Schoeman, M. G.; Meijer, G.; Vergeldt, F. J.; Zuilhof, H.; Sudholter, E. J. R. *Langmuir* **2000**, *16*, 10359–10368.
(33) Foley, E. T.; Yoder, N. L.; Guisinger, N. P.; Hersam, M. C. *Rev. Sci. Instrum.* **2004**, *75*, 5280–5287.
(34) Boyd, R. W. *Nonlinear Optics*, 3rd ed.; Academic Press: New York, 2003.
(35) Shen, Y. R. *The Principles of Nonlinear Optics*; John Wiley & Sons Inc.: Hoboken, NJ, 2003.
(36) Shen, Y. R.; Ostroverkhov, V. *Chem. Rev.* **2006**, *106*, 1140–1154.
(37) Zhu, X. D.; Suhr, H.; Shen, Y. R. *Phys. Rev. B* **1987**, *35*, 3047.
(38) Richter, L. J.; Petralli-Mallow, T. P.; Stephenson, J. C. *Opt. Lett.* **1998**, *23*, 1594–1596.
(39) van der Ham, E. W. M.; Vrehen, Q. H. F.; Eliel, E. R. *Surf. Sci.* **1996**, *368*, 96–101.
(40) Hayes, P. L.; Chen, E. H.; Achtyl, J. L.; Geiger, F. M. *J. Phys. Chem. A* **2009**, *113*, 4269–4280.

system (Spitfire Pro, Spectra Physics, 2.5 mJ/pulse) with a 1 kHz repetition rate was used to pump an optical parametric amplifier (OPA-800CF, Spectra Physics) producing broad-band IR laser light around 3.4 μm with a bandwidth (full-width at half-maximum) of $\sim$140 cm^{-1}. The 800 nm visible beam and IR light were focused onto the sample at incident angles of 45° and 60° from normal, respectively. Following previous work on Si(111),[31] the energy of the visible light was kept between 0.8 and 1.2 μJ to prevent burning of the sample while the IR incident light field ranged from 1.5 to 3.4 μJ. The SFG, visible, and IR beams were all p polarized. Any reflected visible light and light from nonlinear processes besides SFG was filtered out from the generated SF signal, which was then dispersed with a 0.5 m spectrograph (Acton Research) and detected with a liquid nitrogen cooled, back-thinned charged coupled device (CCD) camera (Roper Scientific, 1340 $\times$ 100 pixels^2). All spectra were referenced to the 2962 cm^{-1} methyl asymmetric stretch of an octadecyl monolayer on Si(111).[46] The spectra presented in this work were collected in 1 min, with input IR frequency centered at 3008 cm^{-1}, and averaged over 30 background-subtracted spectra. The spectra were normalized to exhibit the same signal-to-noise ratio, and the nonresonant background was fitted with a Gaussian and subtracted out.

Computational Details. A six-layer Si(100)-2 $\times$ 1 periodic slab geometry was chosen for this study to simulate the substrate environment and molecular chain interactions. The density functional theory (DFT) local density approximation (LDA) was applied in all simulations within the SIESTA[47] electronic structure package. Using a double-ζ-polarized basis and a real space grid sampling of 4082 eV, structures were relaxed through the conjugate gradient method to force tolerance of 0.01 eV/Å.[47,48] To capture surface−molecule interactions, the molecule and top four Si layers of the slab were relaxed while the remaining under layer atoms were frozen at bulk Si lattice coordinates. Periodic interactions along the Si(100)-2 $\times$ 1 surface were captured through *k*-point sampling (at a cutoff of 15 Å).[47] A vacuum region of 10 Å was included to prevent periodic interactions between the top and the bottom of the slab. The simulated STM images were generated through the Tersoff−Hamann approximation.[49] The tunneling local density of states (LDOS) for each system was determined by summing over the substrate eigenstates in the bias energy window.[48] We assume that the substrate Fermi level (E_f) is situated close to the n$^+$−Si conduction band edge (E_C) and considered tunneling at a negative STM bias voltage of −2 V through all states 2 eV below E_f.[48]

Results

UHV STM of PA One-Dimensional Nanostructures. Initial imaging following PA deposition on the Si(100)-2 $\times$ 1:H surface is shown in Figure 1a. The STM images show that the PA molecules form self-assembled one-dimensional nanostructures that are aligned parallel to the underlying silicon dimer rows. While the PA one-dimensional nanostructures share similar characteristics with those previously reported for styrene,[10] they also possess observable differences. For example, the PA one-dimensional nanostructures are typically shorter in length than styrene by approximately a 2:3 ratio for comparable molecular dosing conditions. Furthermore, double chains of PA molecules are not observed to form on the same silicon dimer row.

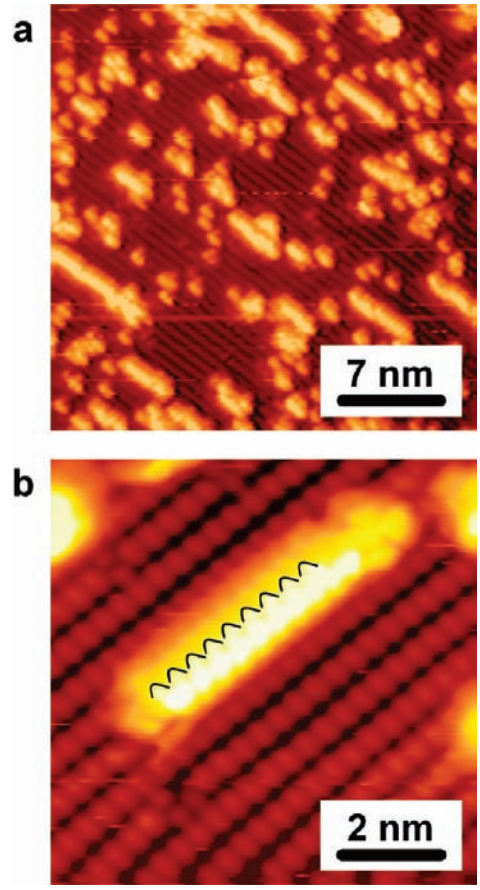

Figure 1. (a) STM image of PA one-dimensional nanostructures on the Si(100)-2 $\times$ 1:H surface. This constant current STM image was taken at a sample bias of −2.0 V and a set point current of 100 pA. (b) High-resolution STM image of one PA nanostructure that consists of nine molecules bound to nine silicon dimers (the black outlines are added to aid the reader in identifying the individual molecules within the nanostructure). This constant current STM image was taken at a sample bias of −1.5 V and with a set point current of 50 pA.

The high-resolution STM image in Figure 1b reveals further details about the alignment of the PA molecules with respect to the underlying silicon dimer row. In particular, the one-dimensional nanostructure in Figure 1b contains nine PA molecules over a length scale that corresponds to nine silicon dimers, thus indicating that there is only one PA molecule bound per silicon dimer. Additionally, while the one-dimensional nanostructure is well aligned and parallel to the silicon dimer row, each constituent PA molecule is offset laterally from the middle of its underlying silicon dimer.

UHV STM of Heteromolecular Nanostructures. In order to directly compare styrene and PA on the Si(100)-2 $\times$ 1:H surface, both molecules were sequentially dosed to form the heteromolecular nanostructure schematically depicted in Figure 2a. Initially, styrene was deposited on the surface, and STM images (Figure 2b) reveal only styrene nanostructures on the surface. A dose of PA is then deposited on the surface, resulting in PA

(41) Konek, C. T.; Illg, K. D.; Al-Abadleh, H. A.; Voges, A. B.; Yin, G.; Musorrafiti, M. J.; Schmidt, C. M.; Geiger, F. M. *J. Am. Chem. Soc.* **2005**, *127*, 15771–15777.
(42) Stokes, G. Y.; Gibbs-Davis, J. M.; Boman, F. C.; Stepp, B. R.; Condie, A. G.; Nguyen, S. T.; Geiger, F. M. *J. Am. Chem. Soc.* **2007**, *129*, 7492–7493.
(43) Voges, A. B.; Al-Abadleh, H. A.; Musorrafiti, M. J.; Bertin, P. A.; Nguyen, S. T.; Geiger, F. M. *J. Phys. Chem. B* **2004**, *108*, 18675–18682.
(44) Voges, A. B.; Stokes, G. Y.; Gibbs-Davis, J. M.; Lettan, R. B.; Bertin, P. A.; Pike, R. C.; Nguyen, S. T.; Scheidt, K. A.; Geiger, F. M. *J. Phys. Chem. C* **2007**, *111*, 1567–1578.
(45) Voges, A. B.; Al-Abadleh, H. A.; Geiger, F. M. In *Environmental Catalysis*; Grassian, V. H., Ed.; Taylor & Francis: Boca Raton, 2005; p 83−128.
(46) Nihonyanagi, S.; Miyamoto, D.; Idojiri, S.; Uosaki, K. *J. Am. Chem. Soc.* **2004**, *126*, 7034–7040.
(47) Soler, J. M.; Artacho, E.; Gale, J. D.; Garcia, A.; Junquera, J.; Ordejon, P.; Sanchez-Portal, D. *J. Phys. Condens. Matter* **2002**, *14*, 2745–2779.
(48) Bevan, K. H.; Zahid, F.; Kienle, D.; Guo, H. *Phys. Rev. B* **2007**, *76*, 045325.
(49) Tersoff, J.; Hamann, D. R. *Phys. Rev. Lett.* **1983**, *50*, 1998–2001.

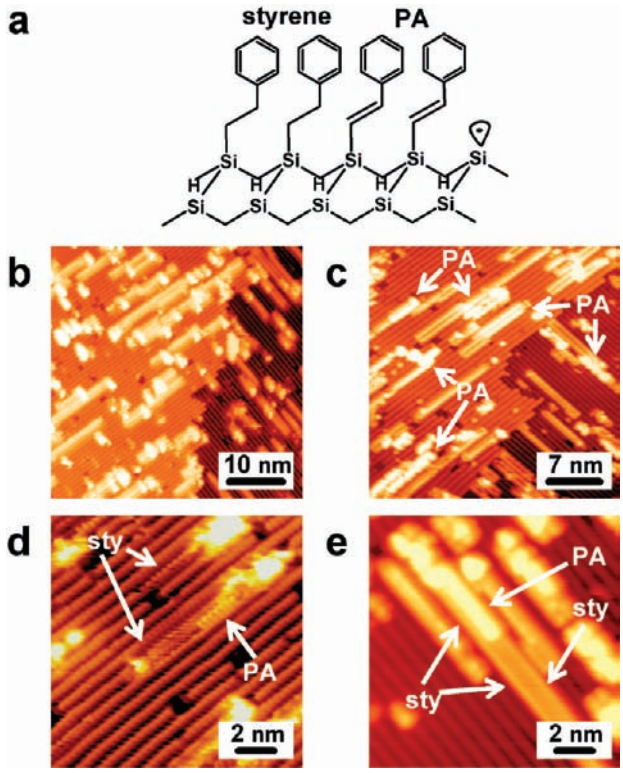

Figure 2. (a) Schematic of the proposed binding configuration for heteromolecular nanostructures formed on the Si(100)-2 × 1:H surface with styrene and PA. (b) STM image (sample bias of −2.2 V and set point current of 200 pA) following a molecular dose of styrene. In this image, only styrene nanostructures are present on the surface. (c) STM image (sample bias of −2.0 V and set point current of 150 pA) following a subsequent molecular dose of PA, leading to the observation of styrene, PA, and heteromolecular nanostructures. The PA nanostructures are labeled in the image and appear taller than the styrene nanostructures. (d) High-resolution STM image (sample bias of −1.8 V and set point current of 150 pA) of heteromolecular nanostructures. The PA molecules appear taller than styrene (labeled "sty"). (e) STM image (sample bias of −2.2 V and set point current of 150 pA) of a double styrene chain, where one side of the chain (the left side) is composed entirely of styrene molecules and the other side (the right side) is composed of both styrene molecules (at the bottom) and PA molecules (at the top).

nanostructure formation. Styrene nanostructures and PA nanostructures are both present on the surface in the resulting STM images (Figure 2c). In some cases the PA nanostructure growth is initiated at a DB at the end of a styrene nanostructure, which results in a heteromolecular nanostructure comprised of both styrene and PA (Figure 2d). In all of these cases, the PA molecules appear taller than styrene in constant current STM images. Since the molecules are expected to possess nearly identical topographic structure, the observed height contrast can likely be attributed to differences in electronic structure.

Unlike styrene one-dimensional nanostructures, no double chains are observed for PA alone. However, Figure 2e reveals an instance of a heteromolecular double-chain nanostructure. In this case, one side of the double chain (the left side) is composed entirely of styrene while the other side (the right side) consists of a block of styrene and a block of PA. Since only one binding site is available per silicon dimer for PA in the heteromolecular double-chain nanostructure, each PA molecule must be bound to the surface via only one silicon atom in this case. It should be noted that the STM image of the PA portion of the double-chain nanostructure appears identical to the other isolated PA nanostructures. Consequently, it can be concluded

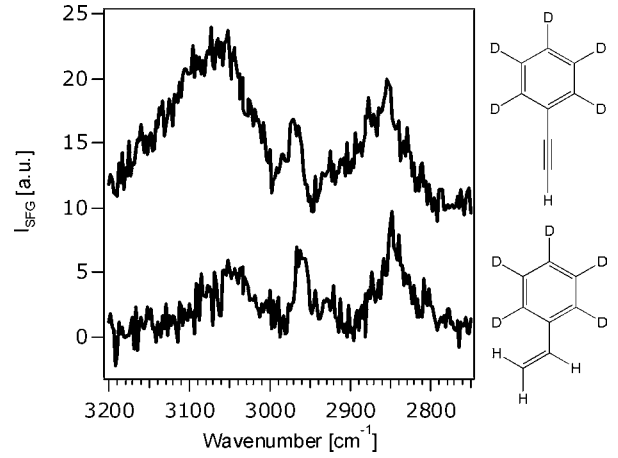

Figure 3. ppp-Polarized SFG spectrum of PA-d5 (top spectrum) and sty-d5 (bottom spectrum) on Si(100)-2 × 1:H recorded with broad-band infrared radiation centered at 3008 cm^{-1}. Each spectrum shown is the average of 30 1-min spectra, with the nonresonant Gaussian background subtracted. The spectra are offset for clarity.

that the PA molecules in single-chain one-dimensional nanostructures are also each bound to only one silicon atom on the surface.

Sum Frequency Generation Measurements. Sum frequency generation (SFG) was used to assess the degree of π-conjugation retention in the surface-bound species formed after chemisorption of PA-d and sty-d to the Si(100)-2 × 1:H surface. As a surface-specific vibrational spectroscopy technique, SFG provides an ideal means for evaluating the hybridization state of the two carbon atoms in a C−C single bond or a C═C double bond, allowing differentiation in the binding motifs for PA and styrene chemisorbed to the Si(100)-2 × 1:H surface. If the terminal alkyne moiety on PA forms a C═C double bond following reaction with Si(100), the chemisorbed species should exhibit a unique spectroscopic signature in the olefinic C−H stretching region (>3000 cm^{-1}).[50,51] Olefinic stretches should be absent in the case of styrene-functionalized Si(100)-2 × 1:H if the vinylic group reacts to form a carbon−carbon single bond with the surface. Thus, SFG is able to track the hybridization state of the organic adlayer. By perdeuterating the five carbon atoms on the phenyl ring, aromatic spectral interference is avoided

The top SFG spectrum displayed in Figure 3 is obtained from averaging 30 ppp-polarized vibrational SFG spectra of PA-d after the nonresonant Gaussian background was subtracted out. A strong broad mode is detected in the olefinic CH stretching region above 3000 cm^{-1}, which is attributed to the terminal C═C double bond because the aromatic C−D stretches on the benzyl ring appear in the 2000−2500 cm^{-1} region.[52] The terminal C═C double bond is expected to be in the trans conformation and exhibit both symmetric and asymmetric CH stretching modes. The broadness of the peak centered at 3060 cm^{-1} can be attributed to the presence of two overlapping vibrational modes or arise from a vibrational resonance interfering with the nonresonant response of the silicon surface. The PA-d spectrum also contains peaks below 3000 cm^{-1}, which are attributed to the well-known combination bands and

(50) Lambert, A. G.; Davies, P. B. *Appl. Spectrosc. Rev.* **2005**, *40*, 103–145.
(51) Hommel, E. L.; Allen, H. C. *The Analyst* **2003**, *128*, 750–755.
(52) Seong, N.-H.; Fang, Y.; Dlott, D. D. *J. Phys. Chem. A* **2009**, *113*, 1445–1452.

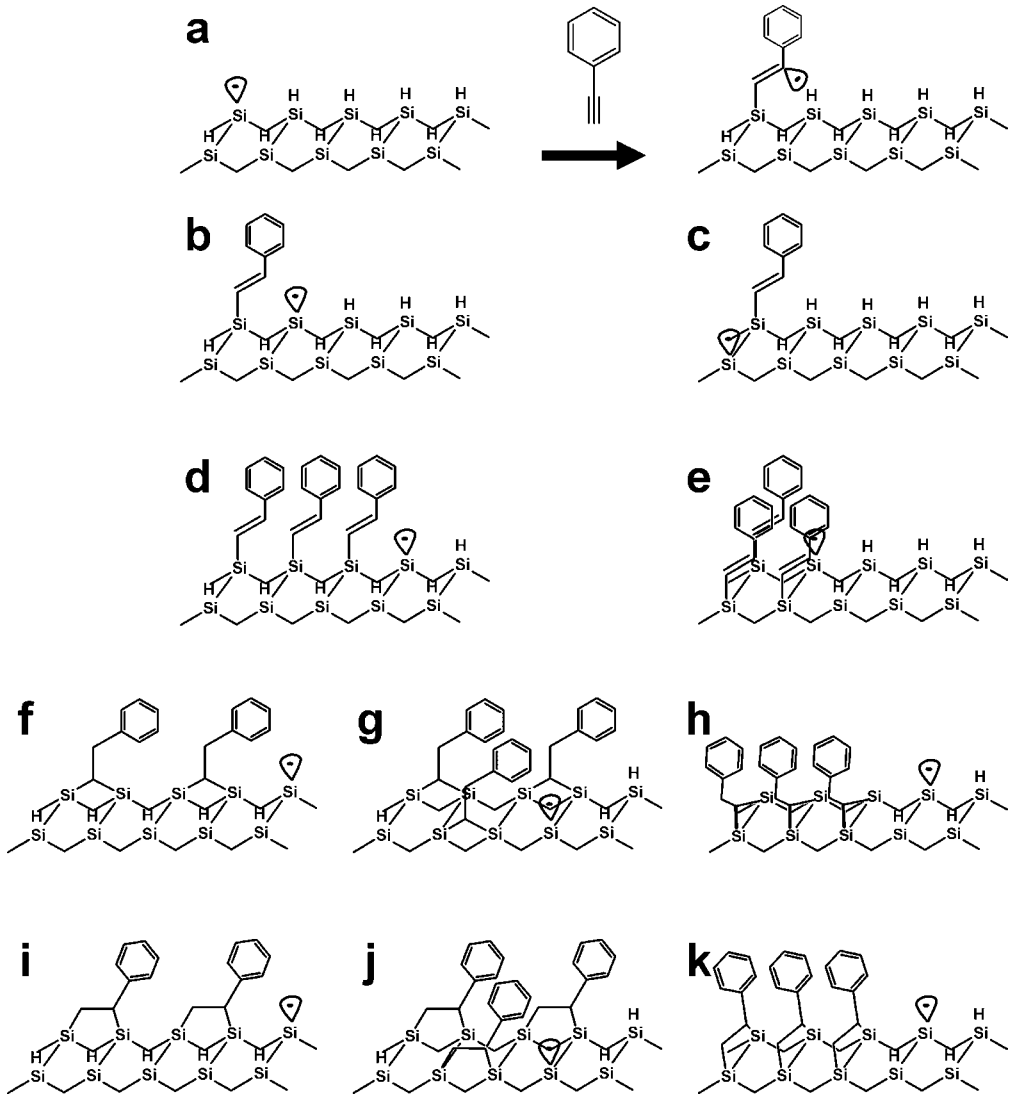

Figure 4. Plausible reaction pathways that yield one-dimensional nanostructures for PA on the Si(100)-2 × 1:H surface. (a) The initial covalent reaction of PA at a silicon DB site creates an alkene carbon radical and subsequent abstraction of a hydrogen atom from either (b) an adjacent silicon dimer or (c) the other side of the same silicon dimer. (d,e) Potential chain reaction pathways where each PA molecule forms only one covalent bond to the silicon surface. (f−h) Potential chain reaction pathways where each PA molecule forms two covalent bonds to the silicon surface in a (1,1) bridge structure. (i−k) Potential chain reaction pathways where each PA molecule forms two covalent bonds to the silicon surface in a (1,2) bridge structure.

overtones that arise from the alkene group and the deuterated phenyl ring.[51,53] Alternatively, the peaks below 3000 cm^{-1} could be due to CH stretches associated with sp^3-hybridized carbon atoms, which would indicate the presence of a small percentage of PA molecules that have reacted with the Si(100)-2 × 1:H surface through processes other than those yielding C═C double bonds. These alternative pathways could include tandem reactions of the terminal alkyne moiety or breaking of the phenyl ring.[54,55] On the basis of UHV STM images of the SFG samples, hydrocarbon contaminants on the surface are ruled out.

Vibrational SFG spectra were also acquired from sty-d-functionalized Si(100)-2 × 1:H. Reaction of the vinylic group on styrene with the Si(100)-2 × 1:H surface yields a terminal C−C single bond, thus disrupting π-conjugation to the surface. The bottom SFG spectrum displayed in Figure 3 confirms the conversion of the vinylic C═C double bond to a C−C single bond based on the SFG signal intensity at 2960 and 2845 cm^{-1}, which correspond to the asymmetric and symmetric methylene modes of the terminal C−C single bond, respectively, or overtones of the d_5-benzyl moiety. The signal intensity above 3000 cm^{-1} for sty-d can be attributed to remaining physisorbed styrene, in which the C═C double bond of the vinyl moiety remains intact. Comparing the vibrational SFG spectra of the Si(100)-2 × 1:H surfaces functionalized with PA-d and sty-d, the SFG signal intensity above 3000 cm^{-1} is substantially higher for PA-d, indicating that the majority of PA-d retains sp^2 hybridization following reaction with the Si(100)-2 × 1:H surface.

Discussion

As mentioned in the Introduction, several reaction pathways have been identified for PA self-assembled monolayers on wet chemically passivated Si(111):H and Si(100):H.[29−32] Consequently, a number of different potential binding configurations

(53) Herzberg, G. *Molecular Spectra and Molecular Structure*; Van Nostrand Reinhold Co.: New York, 1945.
(54) Tao, F.; Qiao, M. H.; Li, Z. H.; Yang, L.; Dai, Y. J.; Huang, H. G.; Xu, G. Q. *Phys. Rev. B* **2003**, *67*, 115334.
(55) Tao, F.; Wang, Z. H.; Lai, Y. H.; Xu, G. Q. *J. Am. Chem. Soc.* **2003**, *125*, 6687–6696.

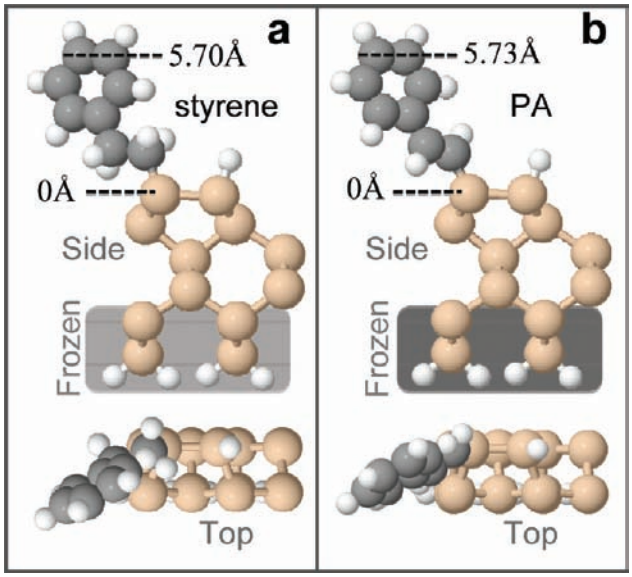

Figure 5. (a) Relaxed coordinates for a periodic unit cell for styrene chemically bound to the Si(100)-2 × 1:H surface indicating a topographic height of 5.70 Å. (b) Relaxed coordinates for a periodic unit cell for PA chemically bound to the Si(100)-2 × 1:H surface indicating a topographic height of 5.73 Å. The two bottom Si layers and back passivating hydrogens are frozen in each relaxation.

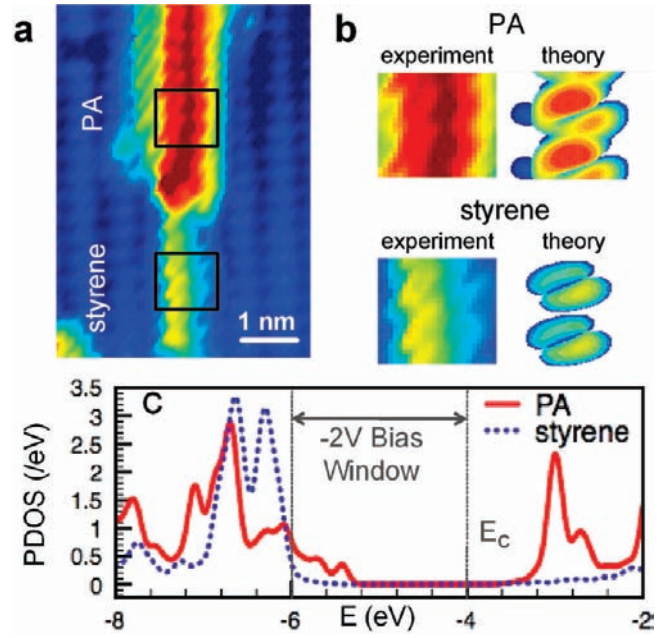

Figure 6. (a) Constant current STM image of a PA and styrene heteromolecular nanostructure taken at −2.0 V sample bias and 150 pA tunneling current. (b) Simulated STM images of PA and styrene nanostructures generated from DFT calculations at an isosurface LDOS value of 10^{-5} e/Bohr^3 are directly compared with the boxed regions of the STM image in Figure 6a. (c) Plot of the projected density of states generated from DFT calculations shows an increase in the number of tunneling states available for PA compared to styrene over the observed bias window.

and reaction pathways are considered here for PA on UHV-prepared Si(100)-2 × 1:H (Figure 4). The high-resolution STM image of Figure 1b revealed that the PA one-dimensional nanostructures possess one PA molecule per silicon dimer, which eliminates the possibilities depicted in Figure 4e, 4f, and 4i. Furthermore, Figure 1b establishes that the PA molecules are offset from the center of the silicon dimer and adjacent PA molecules are aligned along the same side of the silicon dimer row, thus allowing the proposed configurations in Figure 4g and 4j to be disregarded. The heteromolecular double-chain structure observed in Figure 2e shows that the PA molecules only bind to one side of the silicon dimer, which rules out the dimer-bridging structures depicted in Figure 4h and 4k. Consequently, the UHV STM images are only consistent with Figure 4d. In this reaction pathway, the original PA carbon−carbon triple bond covalently reacts with a silicon DB, thus yielding an alkene carbon radical (Figure 4a). This carbon radical subsequently abstracts a hydrogen atom from the neighboring silicon dimer, creating a new DB site (Figure 4b). Prior to any secondary reaction, another PA molecule reacts with the dangling bond and the process is repeated, leading to a one-dimensional chain reaction along one side of the silicon dimer row (Figure 4d). Due to the relatively short observed length of the PA one-dimensional nanostructures (compared to styrene) and the lack of PA double chains, it is likely that a small fraction of the PA molecules do undergo secondary reactions that cause the one-dimensional self-assembly process to terminate prematurely.

Evidently, Figure 4d suggests that the terminal carbon atoms of the chemisorbed PA molecules should possess π-conjugation. Direct evidence for this sp^2 hybridization is found in the UHV STM, SFG, and DFT data. In particular, examining the heteromolecular nanostructures allows the electronic structure of chemisorbed PA and styrene to be directly compared. DFT calculations have been used to interrogate the differences between the two molecular nanostructures. Figure 5 shows the relaxed coordinates for periodic unit cells of styrene and PA. These calculations show that the two molecules possess nearly identical topographic heights (differing by only 0.03 Å) when bound to silicon, which agrees with previously reported results.[31] However, in constant current STM images of PA and styrene, the PA appears taller than styrene by ∼1.2 Å, as seen in Figure 6a. Simulated Tersoff−Hamann (TH) STM images (Figure 6b) compare well with the experimental observations of the heteromolecular chains and predict a constant current height difference of 0.7 Å. Note that the TH approximation generally provides correct trends in STM heights and not exact quantitative values.[48] The simulated STM images corroborate the experimental findings that PA appears distinctly taller in constant current STM images. The STM height difference arises from electronic structure differences between PA and styrene since the topographic difference is negligible.

A plot of the projected molecular density of states (Figure 6c) shows that the observed height difference is due to the larger number of tunneling states available to PA in the −2 V bias window compared with styrene. The experimental observations combined with the DFT calculations are consistent with an electronic structure difference between the two molecules that yields an enhanced tunneling current via the PA compared to styrene. Since extended π-conjugation is known to enhance charge transport through molecular adsorbates,[25] the UHV STM and DFT results of Figure 6 are consistent with the sp^2 hybridization of the PA terminal carbon atoms that is depicted in Figure 4d. Similarly, the vibrational SFG spectra of Figure 3 also reveal the presence of sp^2-hybridized terminal carbon atoms for PA (which is not present for styrene) chemisorbed to the Si(100)-2 × 1:H surface. Overall, the UHV STM, SFG, and DFT data identify Figure 4d as the dominant reaction pathway and binding configuration for the observed PA one-dimensional nanostructures.

Conclusions

In summary, UHV STM, SFG, and DFT have been used to discern the reaction pathway and binding configuration for PA one-dimensional nanostructures on the Si(100)-2 × 1:H surface. UHV STM images following PA molecular dosing of isolated DBs on the Si(100)-2 × 1:H show that PA self-assembles into one-dimensional nanostructures that are aligned parallel to the silicon dimer rows. The one-dimensional nanostructures possess one PA molecule per silicon dimer where adjacent PA molecules are offset in the same direction from the center of the silicon dimer. Further UHV STM characterization of heteromolecular nanostructures consisting of PA and styrene reveal enhanced electronic coupling to the silicon surface for PA compared to styrene. In addition, double-heteromolecular chains establish that each PA molecule possesses only one bond to the silicon surface. Finally, SFG measurements provide direct vibrational spectroscopic evidence for sp^2 hybridization of the terminal carbon atoms for PA chemisorbed to the Si(100)-2 × 1:H surface. Comparison of these experimental results to plausible reaction pathways combined with the DFT calculations strongly suggests that the dominant chemisorbed PA species preserves π-conjugation for the terminal carbon atoms at the silicon surface. Due to their extended π-character, PA one-dimensional nanostructures are promising candidates for molecular electronic and sensing technologies that require strong electronic coupling to silicon surfaces.

Acknowledgment. This work was supported by the National Science Foundation (Award Numbers EEC-0647560, DMR-0520513, and ECS-0506802), the Office of Naval Research (Award Numbers N00014-05-1-0563 and N00014-09-1-0180), and the Department of Energy (Award Number DE-SC0001785). The authors thank Dr. Joseph Lyding for the use of his electronics software and Dr. Lincoln Lauhon for helpful discussions. The authors also acknowledge computational support and resources provided by the National Science Foundation Network for Computational Nanotechnology (Purdue). K.H.B. further acknowledges support from NSERC of Canada (McGill) and support from the DOE under grant no. DE-FG02-05ER46209 and in part by the Division of Materials Sciences and Engineering, Office of Basic Energy Sciences, DOE (ORNL).

JA909139N